Effects of chronic voluntary alcohol consumption on PDE10A availability: a longitudinal behavioural and [^{18}F]JNJ42259152 PET study in rats

Bart de Laat
KU Leuven: Katholieke Universiteit Leuven
Yvonne E. Klingl
VIB KU Leuven Center for Brain & Disease Research: VIB KU Leuven Center for Brain and Disease Research
Gwen Schroyen
KU Leuven: Katholieke Universiteit Leuven
Maarten Ooms
KU Leuven: Katholieke Universiteit Leuven
Jacob M Hooker
Harvard Medical School
Guy Bormans
KU Leuven: Katholieke Universiteit Leuven
Koen Van Laere
UZ Leuven: Katholieke Universiteit Leuven Universitaire Ziekenhuizen Leuven
Jenny Ceccarini (jenny.ceccarini@uzleuven.be)
University Hospitals Leuven and KU Leuven https://orcid.org/0000-0003-2774-9516

Research Article

Keywords: alcohol preference, phosphodiesterase 10A, microPET, [18F]JNJ42259152, open field test, rat Iowa Gambling Task

Posted Date: March 13th, 2021

DOI: https://doi.org/10.21203/rs.3.rs-310567/v1

Abstract

Purpose

Phosphodiesterase 10A (PDE10A) is a dual substrate enzyme highly enriched in dopamine-receptive striatal medium spiny neurons, which are involved in psychiatric disorders such as alcohol use disorders (AUD). Although preclinical studies suggest a correlation of PDE10A mRNA expression in neuronal and behavioral responses to alcohol intake, little is known about the effects of alcohol exposure on *in vivo* PDE10A activity in relation to apparent risk factors for AUD such as decision-making and anxiety.

Methods

We performed a longitudinal [^{18}F]JNJ42259152 microPET study to evaluate PDE10A changes over a 9-week intermittent access to alcohol model, including 6 weeks of alcohol exposure, 2 weeks of abstinence followed by 1 week relapse. Parametric PDE10A binding potential (BP_{ND}) images were generated using a Logan reference tissue model with cerebellum as reference region and were analyzed using both a volume-of-interest and voxel-based approach. Moreover, individual decision-making and anxiety levels were assessed with the rat Iowa Gambling Task and open field test over the IAE model.

Results

We observed an increased alcohol preference especially in those animals that exhibited poor initial decision-making. The first 2-weeks of alcohol exposure resulted in an increased striatal PDE10A binding (> 10%). Comparing PDE10A binding potential after 2- versus 4-weeks of exposure, showed a significant decreased PDE10A in the caudate-putamen and nucleus accumbens ($p_{FWEcorrected}<0.05$). This striatal PDE10A decrease was related to alcohol consumption and preference. Normalization of striatal PDE10A to initial levels was observed after 1 week of relapse, apart from the globus pallidus.

Conclusion

This study shows that chronic voluntary alcohol consumption induces a reversible increased PDE10A enzymatic availability in the striatum, which is related to the amount of alcohol preference. Thus, PDE10A-mediated signaling plays an important role in modulating the reinforcing effects of alcohol, and the data suggest that PDE10A inhibition may have beneficial behavioral effects on alcohol intake.

Introduction

Alcohol use disorders (AUD) have a large impact on the population's mental and physical well-being as they embody chronically relapsing conditions with relapse rates of 40–60%. It is now commonly

accepted that addiction develops through phases, characterized by an initial recreational use, followed by excessive consumption, compulsive drug seeking and episodic withdrawal, and terminates in drug seeking and relapse. However, although the knowledge on the neurobiology of AUD is still expanding, efficacious treatments for AUD are still missing.

Aside from classical targets associated with alcohol-related reward, such as dopaminergic, glutamatergic, mu-opioid and GABAergic neurons [1–3], research is now also focusing on biological substrates responsible for negative reinforcement and chronic relapse, impulse loss of control, dysphoria, anxiety, stress and maladaptive mechanisms resulting from protracted drug use.

Specific subclasses of the phosphodiesterase (PDE) enzyme family are particularly attractive for pharmacological manipulation in respect to drugs of abuse, including alcohol [4]. PDEs are dual specific enzymes which hydrolyze cyclic adenosine and guanosine monophosphate (cAMP and cGMP), consequently regulating cognate signaling pathways such as synaptic plasticity [5], learning, memory and cognition [6, 7] as well as promoting neuronal survival [8]. Several studies suggested the cyclic nucleotide phosphodiesterase-10A (PDE10A) as a promising target when it comes to tackling diseases that have been related with disturbances of striatal dopamine transmission like neurodegenerative and neuropsychiatric disorders [9], due to its high and localized expression in the medium spiny neurons (MSNs) of the basal ganglia [10]. PDE10A is involved in the hydrolysis of the cyclic nucleotides adenosine monophosphate (cAMP) and guanosine monophosphate (cGMP) [11, 12], regulating the excitability of MSNs and thereby acting on the postsynaptic dopaminergic neurotransmission. Both dopamine D1 and D2 receptors mediate their effects through activation or inactivation of the cAMP/PKA (protein kinase A) pathway in the MSNs [13]. PDE10A can thus be seen a key regulator of basal ganglia dopaminergic function [9].

In line with this, several studies have shown that changes in dopamine neurotransmission are related to changes in PDE10A activity [14–16]. Pharmacological inhibition of PDE10A has been shown preclinical and clinical efficacy in movement-related disorders such as Parkinson's and Huntington's diseases [17–22], but also in neuropsychiatric diseases such as schizophrenia [6, 23–25] and substance use disorders [26, 27]. For instance, MP-10, a highly selective PDE10A inhibitor, attenuates morphine-induced conditioned place preference and facilitates extinction in rats [26], similarly to cocaine-induced effects [27].

In AUD, PDE10A has been suggested to also be a regulator of neuronal responses after reinforcement and to alter motivated behaviors like alcohol self-administration. The first connection between PDE10A and AUD was established when PDE10A mRNA expressions in the prelimbic prefrontal cortex showed a correlation with greater alcohol self-administration during the relapse-like phase in rats with a history of stress exposure [28]. Secondly, during protracted withdrawal, PDE10A mRNA levels were reduced in the dorsal striatum, prelimbic prefrontal cortex, and medial amygdala, in contrary to elevated PDE10A mRNA expression observed in the basolateral amygdala during both acute and protracted withdrawal [29]. The same group also showed administration of TP-10, another selective PDE10A inhibitor, was able to reduce

alcohol self-administration in alcohol-dependent and non-dependent rats with or without a history of stress and in genetically alcohol-preferring rats [30].

Whereas there is preclinical evidence to support the involvement of PDE10A in neuronal and behavioral responses to alcohol intake and preference, little is known about the effects of alcohol exposure, abstinence, and relapse on *in vivo* PDE10A enzymatic activity, in relation to apparent risk factors for AUD such as decision-making and anxiety. To address this knowledge gap, we performed a longitudinal [^{18}F]JNJ42259152 PDE10A microPET imaging [31] study, to directly measure *in vivo* changes of PDE10A availability in rats monitored over a 9-week alcohol abuse reinstatement model, mimicking different stages of AUD, in combination with decision-making and anxiety assessments.

Materials And Methods

Animals and procedures

In total 18 adult male Wistar rats (R. Janvier, Le Genest-St-Isle, France), individually housed in a temperature- and humidity-controlled room under an inverse 12-hour light/dark cycle, were investigated (average weight at the time of the experiment: 332 ± 7 g). A subset of 9 experimental animals were monitored over a 9-week intermittent access of ethanol model (described in the following paragraph), including 6 weeks of alcohol exposure, 2 weeks of abstinence followed by 1 week relapse. The other group of 9 rats were included as a sham group (water exposure) to mainly evaluate the differences of chronic alcohol exposure on PDE10A enzymatic activity compared to baseline levels.

Alcohol drinking paradigm

An intermittent access 20% ethanol 2-bottle-choice drinking paradigm, adapted from Simms *et al*. [32], referred to as an ‘intermittent access to ethanol’ (IAE) animal model, was employed to induce alcohol intake as described previously [33]. The IAE animal model is highly relevant to early stages of alcohol abuse and is one of the most prominent animal models used in ethanol research [34]. Every 24 hours the paradigm was changed presenting either 2 drinking bottles, a water and an experimental ethanol solution bottle containing a 20 percent v/v dilution of 99 percent v/v percent stock ethanol (Technisolv, VWR chemicals, Radnor, PA, USA). After 24 hours, both bottles were taken away and replaced by a single water bottle. To avoid side preference bias, drinking bottles were alternated [32] and bottles were weighted 24 hours after delivery. Alcohol consumption and alcohol preference, calculated as the ratio between the solution and water consumption, were used as outcome. After 6 weeks of alcohol exposure, the rats underwent 2 weeks of abstinence phase with access to the bottle of water only. Finally, the rats regained access during a second alcohol exposure period to alcohol for 1 week to mimic relapse. A detailed timeline of the experiment is shown in Fig. 1.

Behavioral testing

Decision-making and anxiety-related behavior were assessed in all experimental animals with the rat Iowa Gambling Task (rIGT) and Open Field Test (OFT) at week 0 (baseline); week 1, 3, 6 (ethanol exposure phase); week 7 and 8 (abstinence phase), and at week 9 (relapse phase) (Fig. 1). Behavioral tests were always executed on the first two days of the week, in the same order, on similar hours throughout the day starting after 3 hours from the last access to the drinking bottles to allow robust comparison between groups.

Rat Iowa Gambling Task (rIGT)

The experimental design was adapted from Zeeb *et al*. [35]. Animals initiated each trial by making a nose-poke response in one of the four illuminated response holes. A response in any illuminated hole turned off all stimulus lights and led to either onset of the tray-light and delivery of reward or the start of a time-out 'punishment' period. Briefly, each hole has its own reward-punishment profile, based on chance of success, reward size equals to number of pellets, and time-out duration. More specifically, the largest reward size could be obtained by solely choosing the (profile = 0.8, 2, 10) response hole, whereas the riskier choice of the (profile = 0.4, 4, 40) option resulted in the smallest reward size. The outcome (decision-making score) was calculated as [(no. pellets rewarded / no. nose-pokes)], with 2 equals to efficient decision making and < 1.8 equals to poor decision making. The reinforcement schedule was designed so that the two-pellet choice was optimal in terms of reward earned per unit time. After a food reward, a response in the food magazine started the next trial, illuminating the four response holes. If animals failed to respond within 10s, the trial was scored as an omission and the tray-light was re-illuminated. Afterwards, animals could start a new trial. Animals received weekly testing sessions and each session lasted 30 minutes. The total number of trials completed, i.e. amount of times an animal successfully poked its nose in an illuminated hole, were analyzed as a fraction of the total pellets received, as a measurement of risk-taking behavior. In low risk-taking behavior, this number approximates two, indicating primarily option two was chosen.

Open Field Test (OFT): Animal´s individual anxiety-related behavior was assessed using the Open Field Test. Each animal was placed in the center of an open field apparatus that consists of a standard circle arena with a diameter of 80 cm, height 31.5 cm, surrounded by a 40 cm rim. The center of the OFT apparatus was defined as > 20 cm apart from the walls. A camera (HD Pro Webcam C920, Logitech International S.A., Lausanne, Switzerland) above the open field apparatus recorded the rat's movements for 10 min, which were analyzed using in-house software calculating the total distance traveled during one session and the average distance to the center of the field during this period. The ratio between the average center distance over the total distance from the edge to the center was used as surrogate marker for anxiety: a lower locomotor activity was interpreted as a more anxious state. To avoid the effects related to habituation to the environment, animals underwent a 3-day 10-min habituation sessions before the initiation of the actual behavioral testing. An in-house script in RStudio (v1.0.143; Boston, MA, USA) calculated averages of these measurements over a period of 10 minutes.

Small animal PET imaging: acquisition and analysis

Small animal PDE10A imaging was performed using [^{18}F]JNJ42259152. [^{18}F]JNJ42259152 was radiolabeled as previously described by Ooms *et al*. [16] The radiotracer was obtained with a radiochemical purity > 98% and an average molar activity of 150 GBq/μmol at the time of injection.

PDE10A scans were performed on a Focus 220 microPET scanner (Siemens Medical Solutions, Knoxville, TN, USA), which has a transaxial resolution of 1.35 mm in full-width at half-maximum. The entire scan, rats were kept under gas anesthesia (2.5 % isoflurane in O_2 at a flow rate of 1 L/min) and on a heating pad at 37°C. Heart rate and breathing rate of all rats were monitored during the entire experiment. Animals were injected intravenously into the tail vein with an average of 24.1 ± 1.9 MBq (23.4 ± 1.8 MBq at the first time point, 24.8 ± 1.8 MBq at the second time point, and 24.0 ± 2.2 MBq at the last time point).

Dynamic 60-minute scans started simultaneously with [^{18}F]JNJ42259152 injection with 3 animals scanned on a single bed at the same time. Data were acquired in a 128 x 128 x 95 matrix with a pixel width of 0.95 mm and a slice thickness of 0.8 mm. List-mode data were reconstructed in 21 time frames (4 x 15 s, 4 x 60 s, 5 x 180 s, 8 x 300 s) for a 60 min acquisition using an iterative maximum *a posteriori* probability algorithm reconstruction and attenuation correction by means of ^{57}Co-attenuation scan. A summed image of the reconstructed data was spatially normalized to a custom-made rat brain template (^{11}C-raclopride) in Paxinos stereotactic space [36], which also has a predominant striatal uptake. The affine transformation was then used to normalize all time frames of the dynamic microPET data set to allow automated and symmetric volumes of interest (VOI) analyses, using a predefined VOI map defined in PMOD (v3.3; PMOD Technologies, Zürich, Switzerland). Parametric PDE10A binding potential (BP_{ND}) images were generated using a Logan reference tissue model with cerebellum as reference region [31, 37], and were analyzed using both a VOI- and voxel-based approach. Parametric PDE10A BP_{ND} images of the 9 rats used as a control sham group [37] to facilitate comparison with the 2-weeks alcohol exposure experimental group, were generated using the acquisition time interval of 60 minutes and were identically processed.

Voxel-wise analyses were performed without *a priori* knowledge of the target regions using Statistical Parametric Mapping 12 (SPM12, Wellcome Department of Cognitive Neurology, London, United Kingdom). After spatial normalization, PDE10A BP_{ND} images were smoothed with a 1.2 mm full width at half maximum Gaussian filter and masked for extracerebral signals. SPM analysis of PDE10A BP_{ND} data was performed with an 80% relative analysis threshold in a flexible factorial design for longitudinal data, and in a categorical design for the control group versus each alcohol condition. T-map thresholds were set at 0.005 uncorrected for the peak voxel level and > 200 voxels for the cluster size (kE). Only clusters that reached significance at $p_{cluster} < 0.05$ (FWE corrected) were retained.

Statistical analysis

Conventional statistics were carried out using GraphPad Prism 8.1.2 software (GraphPad Software Inc., La Jolla, CA, USA). A non-parametric Friedman test followed by a Dunn´s post hoc test was performed to detect differences on the alcohol consumption and alcohol preference across the different weeks of

alcohol exposure. The same statistical test was performed to compare BP_{ND} values at the different time points. An unpaired Mann-Whitney t-test was performed to evaluate BP_{ND} changes in the experimental alcohol group compared to the sham control condition, for both VOI- and voxel-based analysis. The correlation analyses between regional PDE10A changes between the different alcohol conditions and behavioral outcomes were performed using Spearman´s nonparametric test. Data are expressed as the mean ± SEM, and statistical significance was set at $p < 0.05$.

Results

Alcohol consumption and preference

Overall, both alcohol consumption and preference significantly increased over time (alcohol consumption: $\chi^2(6) = 42.77$, $p < 0.0001$; alcohol preference: $\chi^2(6) = 43.39$, $p < 0.0001$). The alcohol consumption significantly escalated at week 3 ($p < 0.05$), as well as at week 6 ($p < 0.0001$) and week 9 (*relapse condition*; $p < 0.0001$) in comparison to the initial intake reported at week 1 (Fig. 2.**a**). Compared to week 1 (average 2.8 ± 0.6 g/kg/day), the rats reached a higher alcohol consumption (76%) after only 3 weeks of administration (4.9 ± 0.7 g/kg/day). After 2 weeks of abstinence, the alcohol consumption remained overall stable (6.0 ± 1.0 g/kg/day) (Fig. 2.**a**). Similarly, alcohol preference (alcohol/water) increased over time with significantly higher preference during week 3 (32 ± 5%; $p < 0.005$) and during the relapse period (33 ± 6%; $p < 0.005$), compared to week 1 (Fig. 2.**b**). Noteworthy, we observed that few rats developed higher alcohol consumption and preference during the first phase of the IAE model, which was maintained or even increased after abstinence.

Behavioral testing

Rat Iowa Gambling Task

Assessing risk-taking behavior during the 9 weeks of alcohol model, the rIGT revealed overall a general constant behavioral performance across the IAE model. The mean decision-making score was 1.90 ± 0.08.

The rats obtained 70 ± 5 rewards consisting of 132 ± 7 pellets in total.
We could not observe significant alcohol-related changes in risk-taking performances ($p = 0.12$). However, when looking at baseline individual rIGT performance, a subgroup of rats scored low ranging from 1.4 to 1.7 (on average 1.6 ± 0.1; Fig. 3.**a**). To evaluate whether individual behavioral baseline characteristics of the animals had an influence on their alcohol consumption, mixed model analysis was performed. The score on the rIGT was shown to significantly predict alcohol consumption over time ($p = 0.017$). When dividing the animals based on the baseline rIGT score (< 1.8 *vs* > 1.8 equals to poor *vs* normal decision making) and displaying their alcohol consumption, a significant difference between the two groups was observed exclusively at baseline ($p < 0.001$). Indeed, the rats scoring low on the baseline rIGT (< 1.8) were those rats who consumed a larger and increasing amount of alcohol per day (Fig. 3.**a**).

Open Field Test

The IAE model displayed an overall main effect on the two OFT outcome automated measures over the different alcohol phases compared to baseline, determined by both the mean total distance travelled ($p < 0.0001$) as well as the distance to the center ($p < 0.0001$), and hence by the resulting center distance/total distance ratio during the 10 min OFT ($p < 0.0001$). This applied to all time points when comparing to baseline (67.4 ± 2.9 cm), resulting in a significant decreased locomotor activity during the 6 weeks of chronic-alcohol intake (33.5 ± 4.5 cm), the abstinence phase (week 7 and 8; 30.6 ± 2.6 cm) and relapse (week 9; 27.5 ± 3.2 cm) (Fig. 3.**b**). The OFT ratio significantly decreased during the relapse phase (reflecting an increased anxious behavior), comparing to week 3 and 6 of alcohol consumption ($p = 0.02$, Fig. 3.**c**). While baseline OFT characteristics could not predict initial alcohol consumption (interaction effects), significant effect of the alcohol consumption on OFT performances was observed during the final alcohol intake period ($p = 0.037$), the first week of abstinence ($p = 0.022$) and relapse (week 9; $p = 0.003$).

PDE10A microPET changes and alcohol exposure

Average PDE10A BP_{ND} maps acquired for the sham control condition and for the experimental IAE condition (after 2, 4 weeks of alcohol exposure, and at relapse after 2 weeks of abstinence) are represented in Fig. 4.**a**. The first 2 weeks of alcohol exposure (ALC w2) resulted in an increased PDE10A binding in the striatum (+ 12%, $p = 0.04$; Fig. 5) and nucleus accumbens (NuAc: +10%), compared to the sham group. Voxel-based comparison between sham and ALC w2 revealed increased PDE10A BP_{ND} values in two clusters comprising the bilateral caudate-putamen ($p_{height} < 0.005$; Fig. 4.**b**).

Comparing PDE10A BP_{ND} after 4- versus 2-weeks of exposure, showed a decreased PDE10A binding in the bilateral caudate-putamen, extending to the NuAc shell and bed nucleus of the stria terminalis ($P_{FWEcorrected}$: 0.02 – 0.003, $T_{peak} > 3.6$, Fig. 4.**c**; VOI-based: striatum: -14%, $\chi^2(2) = 8.22$, $p = 0.02$; NuAc: -17%, $\chi^2(2) = 8.67$, $p = 0.01$).

A similar regional decrease in PDE10A availability towards normalization was observed after two weeks of abstinence, extending to the lateral globus pallidum ($P_{FWE-corrected}$: 0.002–0.008, $T_{peak} > 3.8$, Fig. 4.**c**; VOI-based: striatum: -17%, $p = 0.02$; NuAc: -22%, $p = 0.01$). After one week of relapse, VOI-based analysis confirmed this PDE10A augmentation back to PDE10A binding at sham condition in the striatum ($p = 0.19$) and NuAc ($p = 0.14$). VOI- and voxel-based analyses showed that the decreased PDE10A availability in the lateral globus pallidum at week 2 of alcohol exposure tends to further decrease at week 4 and relapse, extending to the bed nucleus of the stria terminalis ($p_{height} < 0.005$; mean decrease = − 29 ± 14% at Paxinos coordinate: x = 3.0, y = -0.9, z = 5.8; VOI-based: $p = 0.004$, see Fig. 4 and Fig. 5).

This striatal PDE10A decrease was mostly present in high-alcohol preferring rats (in average, striatum: -21.2%; NuAc: -27.6%), compared to the low-alcohol preferring rats (striatum: -6.2%; NuAc: -6.7%) (**Supplemental Fig. 1**). The observed alcohol-induced striatal PDE10A changes were not related to rIGT

performances at any time point of the alcohol model. It is nevertheless noteworthy that no significant alcohol-related changes in risk-taking performances were observed over time (see Fig. 3.**a**). However, comparing the percentage changes of the OFT locomotor activity over the different alcohol phases with individual baseline performances, we found negative correlations between PDE10A binding changes in the NuAc at week 4 of alcohol exposure and during relapse and decrease in OFT locomotor activity at the initial and final phase of the alcohol model (alcohol week 1: r_s = -0.7; p = 0.043; relapse period week 9: r_s = -0.65; p = 0.05).

Discussion

In the current preclinical study, we combined longitudinal behavioral paradigms with longitudinal PDE10A microPET imaging, to directly evaluate *in vivo* changes of PDE10A activity in rats during different stages of AUD, in combination with behavioral assessments such as anxiety and decision-making. Overall, we found that two weeks of voluntary alcohol consumption induced a reversible increased PDE10A enzymatic availability in the dorsal and ventral striatum. At both week 4 of the alcohol exposure and relapse, the striatal PDE10A decrease was related to alcohol consumption and preference. Also, the rats who showed a greater future alcohol intake corresponded to those rats with an initial impaired decision-making and a lower locomotor activity, possibly due to a more anxious state, during the abstinence and relapse phase.

To induce alcohol consumption in our experimental group of rats, we used the IAE model with a 2-bottle choice paradigm, one of the most prominent and validated animal models used in ethanol research nowadays [32, 34]. The IAE model successfully induced an escalation in alcohol consumption after the first weeks of alcohol administration, following the threshold criteria of high ethanol consumption (> 4.5 g/kg/day) suggested by Carnicella *et al*. [38]. Moreover, after the two weeks of abstinence, the average alcohol intake returned to the same level as before the period of abstinence, suggesting that IAE paradigm induces adaptations which are maintained after abstinence, in line with previous findings [32, 38]. However, although half of the group did not exploit high alcohol consumption during the first intake phase, observing the progress of the individual ethanol intake, a subgroup of rats clearly developed high alcohol consumption over time. So far, little is known about the predisposing behavioral traits of high alcohol intake in rats, except rats with higher impulsivity traits are known to have a higher alcohol intake [39]. Noteworthy, in this study a low baseline rIGT performance, hence impaired initial decision-making, are related to an higher alcohol consumption over time. When looking at behavioral outcomes in function of the alcohol exposure over time; six weeks of alcohol intake had no effects on decision-making performances, while on the other hand a decreased locomotor activity (hence increased anxious behavior) was found starting from week 3 on, including the abstinence and relapse period.

Regarding alcohol consumption and PDE10A availability over time, our longitudinal [^{18}F]JNJ42259152 PDE10A imaging data showed that two weeks of voluntary alcohol consumption induced an increased PDE10A enzymatic availability in the striatum and NuAc. We also found that this alcohol-induced PDE10A upregulation was reversible upon a longer period of alcohol administration and was mostly

present in those rats that consumed a bigger amount of alcohol. A similar regional decrease in PDE10A availability towards normalization was observed after one week of relapse, extending to the lateral globus pallidum.

The observed PDE10A changes might be a result of alterations in dopamine neurotransmission and subsequent PDE10A modulation through feedback on the cAMP/PKA pathway. PDEs can promote alcohol intake through reduction of cyclic nucleotide activity [40]. Considering the limited distribution of PDE10A to the striatal GABAergic MSNs, together with the role of PDE10A in cAMP-PKA-DARPP-32 signaling cascade and metabolism in the MSNs, several studies have demonstrated a relation between abnormal striatal dopaminergic transmission characterizing neurodegenerative and neuropsychiatric basal ganglia diseases and the loss of PDE10A enzyme levels and expression [18, 21–23, 27]. Upregulated striatal signaling, is PDE10A-regulated in processes controlling reward-motivated behaviors and furthermore, incentive salience [41]. In the striatum the increased dopamine release upon alcohol exposure stimulates both the dopamine D1 and D2 receptor pathways in the postsynaptic density of the MSNs resulting in increased (via D1) or decreased (D2) cAMP levels. It is of central question whether our findings are mostly a consequence of increased stimulation of the direct D1 pathway, or via the opposite indirect D2 pathway resulting in the activation of $G\alpha_{i/o}$, and cAMP inhibition. Ooms et al. [16] observed increased PDE10A binding after repeated D-amphetamine treatment, suggesting a potential pharmacological interaction between PDE10A enzymes and drugs modifying dopamine neurotransmission. This was suggested to be a compensation mechanism secondary to alterations of cAMP-levels being caused by increased D1 receptor stimulation over D2 stimulation. Here, we showed that PDE10A availability in the striatum and NuAc increases at the first stage of alcohol exposure (week 2) and then gradually decreases. This might indicate a short-term neuronal adaptation due to alcohol-induced increased dopamine release, which results in increased stimulation of adenylyl cyclase and thus increased cAMP levels. The MSNs react to increased cAMP levels by up-regulating cyclic nucleotide hydrolyzing enzymes. As a consequence, this leads to an increased PDE10A enzymatic availability that subsequently decreases cAMP levels. Due to the long-term chronic alcohol effect, dopamine release decreases leading to less cAMP production and to a loss of PDE10A. Since we did not observe an increased PDE10A availability during the relapse phase after abstinence, this suggests neuroadaptational changes within specific neurocircuits take place in a long-term fashion.

Preclinical studies suggested that pharmacological inhibition of PDE10A activity with TP-10 dose-dependently reduce alcohol self-administration in rats with stress history, alcohol dependence, or genetic predisposition to high levels of alcohol intake [30]. This action may result, at least partially, from modulation of PDE10A activity in the dorsolateral striatum (DLS), the region that showed a non-recovered PDE10A loss in our findings. Furthermore, systemic TP-10 administration significantly increased dopamine turnover in the DLS and NuAc, with greater potency in the DLS [42]. Consistently, PDE10A inhibition reduces intake of highly palatable high-fat diets in mice [43], supporting PDE10A is involved in the motivational regulation of highly reinforcing substances.

Our findings suggest that it may be a therapeutic target of interest at the initial stage of AUD. Further research is required to advance our understanding of these findings. There is no increase in PDE10A signal after relapse and therefore, we hypothesize an irreversible neuroadaptational change has taken place due to the MSNs down-regulating cyclic nucleotide hydrolyzing enzymes, such as PDE10A. This provides further insight into the molecular mechanisms that are at play in alcoholism and that are so crucial to be fully understood in order to tackle alcoholism as a disease.

The negative emotional state that arises during acute abstinence from alcohol exposure includes elevations in anxiety-like behavior [44]. Previous studies showed that PDE10A may mediate the relation between stress history and elevated relapse risk [28]. Papaverine, a PDE10A inhibitor, has been shown to reduce anxiety-like behavior [45]. Stress history differentially increased PDE10A expression in low versus high drinking rats, with greater PDE10A expression in the prefrontal cortex correlating with greater relapse-like alcohol intake, and greater PDE10A expression in the basolateral amygdala correlating with increased alcohol preference ratios in rats [28]. In agreement with these findings, our results showed that those rats with decreased locomotor activity over the first initial alcohol and relapse phase and therefore, increased anxiety levels, displayed reduced PDE10A changes during both the protracted alcohol exposure (4 weeks) and relapse. This indicates elevated PDE10A levels are associated with heightened anxiety-like behavior. On the other hand, anxiety is a complex collection of behaviours and aspects that cannot be entirely captured by a single test. Although it would be interesting to confirm our findings using other testing, such as the elevated plus maze (EPM) or the light/dark boxes (LDB). Factor analyses revealed that similar anxiety- and locomotion-related factors were produced by the three tests OFT, EPM and LDB applied either separately or in combination [46].

A limitation of our study is the small group size of animals used in this study. Increasing the number of animals would help to improve characterization of the subgroups divided by high and low alcohol consumption. Another potential limitation is the lack of the pre-exposure baseline PDE10A measurements, resulting in only limited information on studying the dynamics of PDE10A changes occurring during exposure to alcohol. Nevertheless, a sham control group scanned under the same conditions was used to investigate the effect of chronic alcohol administration.

Finally, although sham animals were not subjected to behavioral tasks, limiting therefore the interpretability of the current behavioral data, the validation of both OFT and rIGT tests was obtained in a FDG PET sub-study (data not shown).

To our knowledge, this is the first PDE10A microPET study investigating *in vivo* changes of PDE10A activity in rats during different stages of AUD, in relation to apparent risk factors for AUD such as decision-making and anxiety. Our findings indicate that chronic alcohol consumption induces a reversible increased PDE10A enzymatic availability in the striatum that is related to higher alcohol preference. Secondly, we showed that poor decision-making (i.e. high risk-taking and gambling-prone behavior) may be a predisposing factor for a higher vulnerability towards alcohol abuse and AUD, and decreased locomotor activity (i.e. increased anxiety) may be a consequence of chronic alcohol use. Thus, PDE10A-

mediated signaling plays an important role in modulating the reinforcing effects of alcohol, and the data suggest that PDE10A inhibition may have beneficial behavioral effects on alcohol intake.

Abbreviations

AUD: alcohol use disorders; BP: binding potential; cAMP: cyclic adenosine monophosphate; cGMP: cyclic guanosine monophosphate; D1, dopamine receptor type 1; D2: dopamine receptor type 2; IAE: intermittent access to ethanol; MSNs: medium spiny neurons; NuAc: nucleus accumbens; OFT: Open Field Test; PDE: phosphodiesterase; PDE10A: phosphodiesterase 10A; rIGT: rat Iowa Gambling Task; VOI: volumes of interest.

Declarations

Ethics approval and consent to participate: All animal experiments were conducted according to the European Communities Council Directive of November 24, 1986 (86/609/EEC) and approved by the Animal Ethics Committees of the University of Leuven.

Availability of data and materials: Please contact the authors for data request.

Competing interests: The authors declare that they have no competing interests to report in relation to this work.

Funding: This work was funded by a research grant to JC from the Research Foundation Flanders (FWO/1508415N). JC is a postdoctoral fellow from FWO (FWO/12R1619N). YEK is a SB PhD fellow at FWO (FWO/1S50320N), BdL received a PhD fellowship from the Flemish Agency for Innovation by Science and Technology, and KVL is senior clinical research fellow for the FWO. GS, MO, JMH, and GB have no competing financial interests to report in relation to this work.

Authors contributions: The experimental setup was designed by BdL and JC. BdL, GS and MO performed data collection. Data analysis was conducted by YEK and JC. The manuscript was written by YEK and JC, supported by BdL, GS, MO, JMH, GB and KVL. All authors revised the manuscript and accepted the final version.

Acknowledgements: The authors would like to thank Tinne Buelens and Ann Van Santvoort for their excellent technical assistance and the local radiopharmacy team for the tracer productions.

References

1. Leurquin-Sterk G, Ceccarini J, Crunelle CL, Weerasekera A, de Laat B, Himmelreich U, et al. Cerebral dopaminergic and glutamatergic transmission relate to different subjective responses of acute alcohol intake: an in vivo multimodal imaging study. Addiction Biology. Wiley/Blackwell (10.1111); 2018;23:931–44.

2. de Laat B, Weerasekera A, Leurquin-Sterk G, Gsell W, Bormans G, Himmelreich U, et al. Effects of alcohol exposure on the glutamatergic system: a combined longitudinal ^{18} F-FPEB and ^{1} H-MRS study in rats. Addiction Biology. Wiley/Blackwell (10.1111); 2018;
3. Xiao C, Ye JH. Ethanol dually modulates GABAergic synaptic transmission onto dopaminergic neurons in ventral tegmental area: Role of μ-opioid receptors. Neuroscience. 2008;153:240–8.
4. Logrip ML. Phosphodiesterase regulation of alcohol drinking in rodents. Alcohol. Elsevier; 2015;49:795–802.
5. Sanderson TM, Sher E. The role of phosphodiesterases in hippocampal synaptic plasticity. Neuropharmacology. 2013;74:86–95.
6. García-Barroso C, Ugarte A, Martínez M, Rico AJ, Lanciego JL, Franco R, et al. Phosphodiesterase Inhibition in Cognitive Decline. de la Torre JC, editor. Journal of Alzheimer's Disease. 2014;42:S561–73.
7. Peng S, Sun H, Zhang X, Liu G, Wang G. Effects of Selective Phosphodiesterases-4 Inhibitors on Learning and Memory: A Review of Recent Research. Cell Biochemistry and Biophysics. 2014;70:83–5.
8. Kranz K, Warnecke A, Lenarz T, Durisin M, Scheper V. Phosphodiesterase Type 4 Inhibitor Rolipram Improves Survival of Spiral Ganglion Neurons In Vitro. Sokolowski B, editor. PLoS ONE. 2014;9:e92157.
9. Wilson L, Brandon N. Emerging Biology of PDE10A. Current Pharmaceutical Design. 2014;21:378–88.
10. Seeger TF, Bartlett B, Coskran TM, Culp JS, James LC, Krull DL, et al. Immunohistochemical localization of PDE10A in the rat brain. Brain Research. Elsevier; 2003;985:113–26.
11. Jäger R, Russwurm C, Schwede F, Genieser H-G, Koesling D, Russwurm M. Activation of PDE10 and PDE11 phosphodiesterases. The Journal of biological chemistry. American Society for Biochemistry and Molecular Biology; 2012;287:1210–9.
12. Gross-Langenhoff M, Hofbauer K, Weber J, Schultz A, Schultz JE. cAMP is a ligand for the tandem GAF domain of human phosphodiesterase 10 and cGMP for the tandem GAF domain of phosphodiesterase 11. The Journal of biological chemistry. American Society for Biochemistry and Molecular Biology; 2006;281:2841–6.
13. Nishi A, Kuroiwa M, Miller DB, O'Callaghan JP, Bateup HS, Shuto T, et al. Distinct roles of PDE4 and PDE10A in the regulation of cAMP/PKA signaling in the striatum. The Journal of neuroscience : the official journal of the Society for Neuroscience. Society for Neuroscience; 2008;28:10460–71.
14. Dlaboga D, Hajjhussein H, O'Donnell JM. Chronic haloperidol and clozapine produce different patterns of effects on phosphodiesterase-1B, -4B, and -10A expression in rat striatum. Neuropharmacology. Pergamon; 2008;54:745–54.
15. Giorgi M, Melchiorri G, Nuccetelli V, D'Angelo V, Martorana A, Sorge R, et al. PDE10A and PDE10A-dependent cAMP catabolism are dysregulated oppositely in striatum and nucleus accumbens after

lesion of midbrain dopamine neurons in rat: A key step in parkinsonism physiopathology. Neurobiology of Disease. Academic Press; 2011;43:293–303.

16. Ooms M, Celen S, De Hoogt R, Lenaerts I, Liebregts J, Vanhoof G, et al. Striatal phosphodiesterase 10A availability is altered secondary to chronic changes in dopamine neurotransmission. EJNMMI radiopharmacy and chemistry. Springer; 2017;1:3.
17. Niccolini F, Foltynie T, Reis Marques T, Muhlert N, Tziortzi AC, Searle GE, et al. Loss of phosphodiesterase 10A expression is associated with progression and severity in Parkinson's disease. Brain. Narnia; 2015;138:3003–15.
18. Pagano G, Niccolini F, Wilson H, Yousaf T, Khan NL, Martino D, et al. Comparison of phosphodiesterase 10A and dopamine transporter levels as markers of disease burden in early Parkinson's disease. Movement Disorders. John Wiley & Sons, Ltd; 2019;mds.27733.
19. Beaumont V, Zhong S, Lin H, Xu W, Bradaia A, Steidl E, et al. Phosphodiesterase 10A Inhibition Improves Cortico-Basal Ganglia Function in Huntington's Disease Models. Neuron. Cell Press; 2016;92:1220–37.
20. Wilson H, Niccolini F, Haider S, Marques TR, Pagano G, Coello C, et al. Loss of extra-striatal phosphodiesterase 10A expression in early premanifest Huntington's disease gene carriers. Journal of the Neurological Sciences. Elsevier; 2016;368:243–8.
21. Koole M, Van Laere K, Ahmad R, Ceccarini J, Bormans G, Vandenberghe W. Brain PET imaging of phosphodiesterase 10A in progressive supranuclear palsy and Parkinson's disease. Movement Disorders. 2017;32.
22. Ahmad R, Bourgeois S, Postnov A, Schmidt ME, Bormans G, Van Laere K, et al. PET imaging shows loss of striatal PDE10A in patients with Huntington disease. Neurology. Wolters Kluwer Health, Inc. on behalf of the American Academy of Neurology; 2014;82:279–81.
23. Persson J, Szalisznyó K, Antoni G, Wall A, Fällmar D, Zora H, et al. Phosphodiesterase 10A levels are related to striatal function in schizophrenia: a combined positron emission tomography and functional magnetic resonance imaging study. European Archives of Psychiatry and Clinical Neuroscience. Springer Berlin Heidelberg; 2019;1–9.
24. Bodén R, Persson J, Wall A, Lubberink M, Ekselius L, Larsson E-M, et al. Striatal phosphodiesterase 10A and medial prefrontal cortical thickness in patients with schizophrenia: a PET and MRI study. Translational Psychiatry. Nature Publishing Group; 2017;7:e1050–e1050.
25. Chappie T, Humphrey J, Menniti F, Schmidt C. PDE10A inhibitors: an assessment of the current CNS drug discovery landscape. Current opinion in drug discovery & development. 2009;12:458–67.
26. Mu Y, Ren Z, Jia J, Gao B, Zheng L, Wang G, et al. Inhibition of phosphodiesterase10A attenuates morphine-induced conditioned place preference. Molecular Brain. BioMed Central; 2014;7:70.
27. Liddie S, Anderson KL, Paz A, Itzhak Y. The effect of phosphodiesterase inhibitors on the extinction of cocaine-induced conditioned place preference in mice. Journal of Psychopharmacology. 2012;26:1375–82.

28. Logrip ML, Zorrilla EP. Stress history increases alcohol intake in relapse: relation to phosphodiesterase 10A. Addiction biology. NIH Public Access; 2012;17:920–33.
29. Logrip ML, Zorrilla EP. Differential changes in amygdala and frontal cortex Pde10a expression during acute and protracted withdrawal. Frontiers in Integrative Neuroscience. Frontiers; 2014;8:30.
30. Logrip ML, Vendruscolo LF, Schlosburg JE, Koob GF, Zorrilla EP. Phosphodiesterase 10A regulates alcohol and saccharin self-administration in rats. Neuropsychopharmacology : official publication of the American College of Neuropsychopharmacology. Nature Publishing Group; 2014;39:1722–31.
31. Celen S, Koole M, Ooms M, De Angelis M, Sannen I, Cornelis J, et al. Preclinical evaluation of [18F]JNJ42259152 as a PET tracer for PDE10A. NeuroImage. Academic Press; 2013;82:13–22.
32. Simms JA, Steensland P, Medina B, Abernathy KE, Chandler LJ, Wise R, et al. Intermittent access to 20% ethanol induces high ethanol consumption in Long-Evans and Wistar rats. Alcoholism, clinical and experimental research. NIH Public Access; 2008;32:1816–23.
33. Laat B, Weerasekera A, Leurquin-Sterk G, Gsell W, Bormans G, Himmelreich U, et al. Effects of alcohol exposure on the glutamatergic system: a combined longitudinal 18F-FPEB and 1H-MRS study in rats. Addiction Biology. John Wiley & Sons, Ltd (10.1111); 2019;24:696–706.
34. Kimbrough A, Kim S, Cole M, Brennan M, George O. Intermittent access to ethanol drinking facilitates the transition to excessive drinking after chronic intermittent ethanol vapor exposure. Alcoholism, clinical and experimental research. NIH Public Access; 2017;41:1502.
35. Zeeb FD, Robbins TW, Winstanley CA. Serotonergic and Dopaminergic Modulation of Gambling Behavior as Assessed Using a Novel Rat Gambling Task. Neuropsychopharmacology. Nature Publishing Group; 2009;34:2329–43.
36. Casteels C, Vermaelen P, Nuyts J, Van Der Linden A, Baekelandt V, Mortelmans L, et al. Construction and evaluation of multitracer small-animal PET probabilistic atlases for voxel-based functional mapping of the rat brain. Journal of nuclear medicine : official publication, Society of Nuclear Medicine. 2006;47:1858–66.
37. Ooms M, Attili B, Celen S, Koole M, Verbruggen A, Van Laere K, et al. [18F]JNJ42259152 binding to phosphodiesterase 10A, a key regulator of medium spiny neuron excitability, is altered in the presence of cyclic AMP. Journal of Neurochemistry. John Wiley & Sons, Ltd (10.1111); 2016;139:897–906.
38. Carnicella S, Ron D, Barak S. Intermittent ethanol access schedule in rats as a preclinical model of alcohol abuse. Alcohol. Elsevier; 2014;48:243–52.
39. Poulos CX, Le AD, Parker JL. Impulsivity predicts individual susceptibility to high levels of alcohol self-administration. Behavioural pharmacology. 1995;6:810–4.
40. Wen RT, Zhang FF, Zhang HT. Cyclic nucleotide phosphodiesterases: potential therapeutic targets for alcohol use disorder. Psychopharmacology. Springer Verlag; 2018. p. 1793–805.
41. Piccart E, De Backer J-F, Gall D, Lambot L, Raes A, Vanhoof G, et al. Genetic deletion of PDE10A selectively impairs incentive salience attribution and decreases medium spiny neuron excitability. Behavioural Brain Research. Elsevier; 2014;268:48–54.

42. Schmidt CJ, Chapin DS, Cianfrogna J, Corman ML, Hajos M, Harms JF, et al. Preclinical Characterization of Selective Phosphodiesterase 10A Inhibitors: A New Therapeutic Approach to the Treatment of Schizophrenia. Journal of Pharmacology and Experimental Therapeutics. 2008;325:681–90.
43. Nawrocki AR, Rodriguez CG, Toolan DM, Price O, Henry M, Forrest G, et al. Genetic deletion and pharmacological inhibition of phosphodiesterase 10A protects mice from diet-induced obesity and insulin resistance. Diabetes. American Diabetes Association; 2014;63:300–11.
44. Zhao Y, Weiss F, Zorrilla EP. Remission and Resurgence of Anxiety-Like Behavior Across Protracted Withdrawal Stages in Ethanol-Dependent Rats. Alcoholism: Clinical and Experimental Research. John Wiley & Sons, Ltd (10.1111); 2007;31:1505–15.
45. Grauer SM, Pulito VL, Navarra RL, Kelly MP, Kelley C, Graf R, et al. Phosphodiesterase 10A inhibitor activity in preclinical models of the positive, cognitive, and negative symptoms of schizophrenia. The Journal of pharmacology and experimental therapeutics. 2009;331:574–90.
46. Ramos A, Pereira E, Martins GC, Wehrmeister TD, Izídio GS. Integrating the open field, elevated plus maze and light/dark box to assess different types of emotional behaviors in one single trial. Behavioural Brain Research. Behav Brain Res; 2008;193:277–88.

Figures

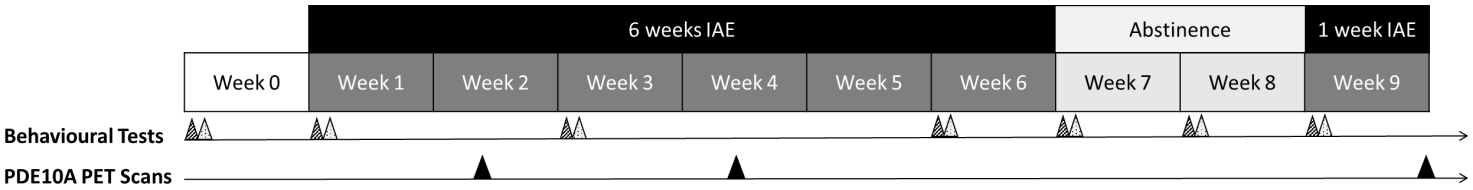

Figure 1

Schematic overview of the experimental design. Time-course of the 9 weeks of the intermittent access of ethanol (IAE) animal model, indicating the time points of the behavioral tests (gray triangle with black stripes for Open Field Test [OFT], white triangle with black points for rat Iowa Gambling Task [rIGT]) and PDE10A microPET scans (black triangle).

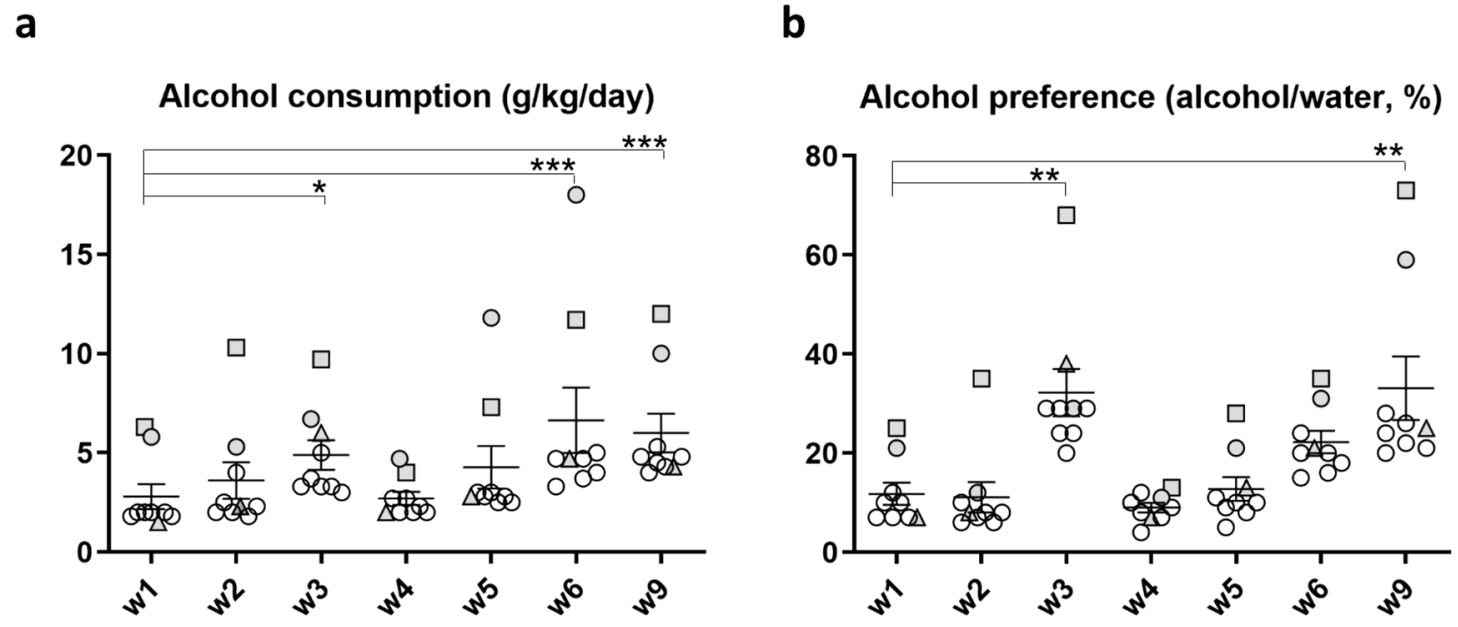

Figure 2

Alcohol consumption and preference in function of the alcohol exposure week. Aligned dot plots (mean ± SEM) showing weekly (a) average alcohol (g/kg /day) consumption and (b) alcohol preference (%, ratio of volume alcohol solution/water intake) over a period of 9 weeks of the intermittent access of ethanol (IAE) animal model. Filled grey symbols show those rats who reported a higher alcohol consumption above the mean during at week 3 of the IAE model. W = week; * $p < 0.05$; ** $p < 0.005$; *** $p < 0.0001$ (Dunn's nonparametric comparison for post hoc Friedman test)

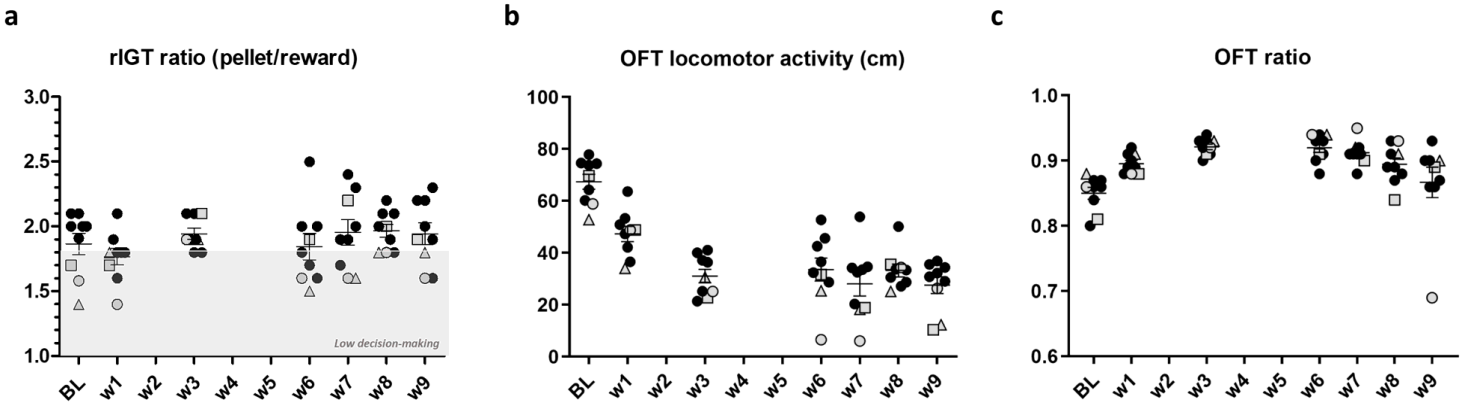

Figure 3

Behavioral outcome (rat Iowa Gambling Task [rIGT] and Open Field Test [OFT]) in function of the alcohol exposure week and alcohol consumption. Aligned dot plots (mean ± SEM) showing the weekly (a) mean ratio of rewards/pellets for the rat Iowa Gambling Task (rIGT) measuring the decision-making and risk-taking, (b) the mean total distance (in cm), and (c) center distance/total distance ratio traveled during the 10 minutes OFT, over a period of 9 weeks of the intermittent access of ethanol (IAE) animal model. The

grey symbols correspond to the same rats who reported a high alcohol consumption and preference during the first IAE phase. * p < 0.05 Dunn's nonparametric comparison for post hoc Friedman test.

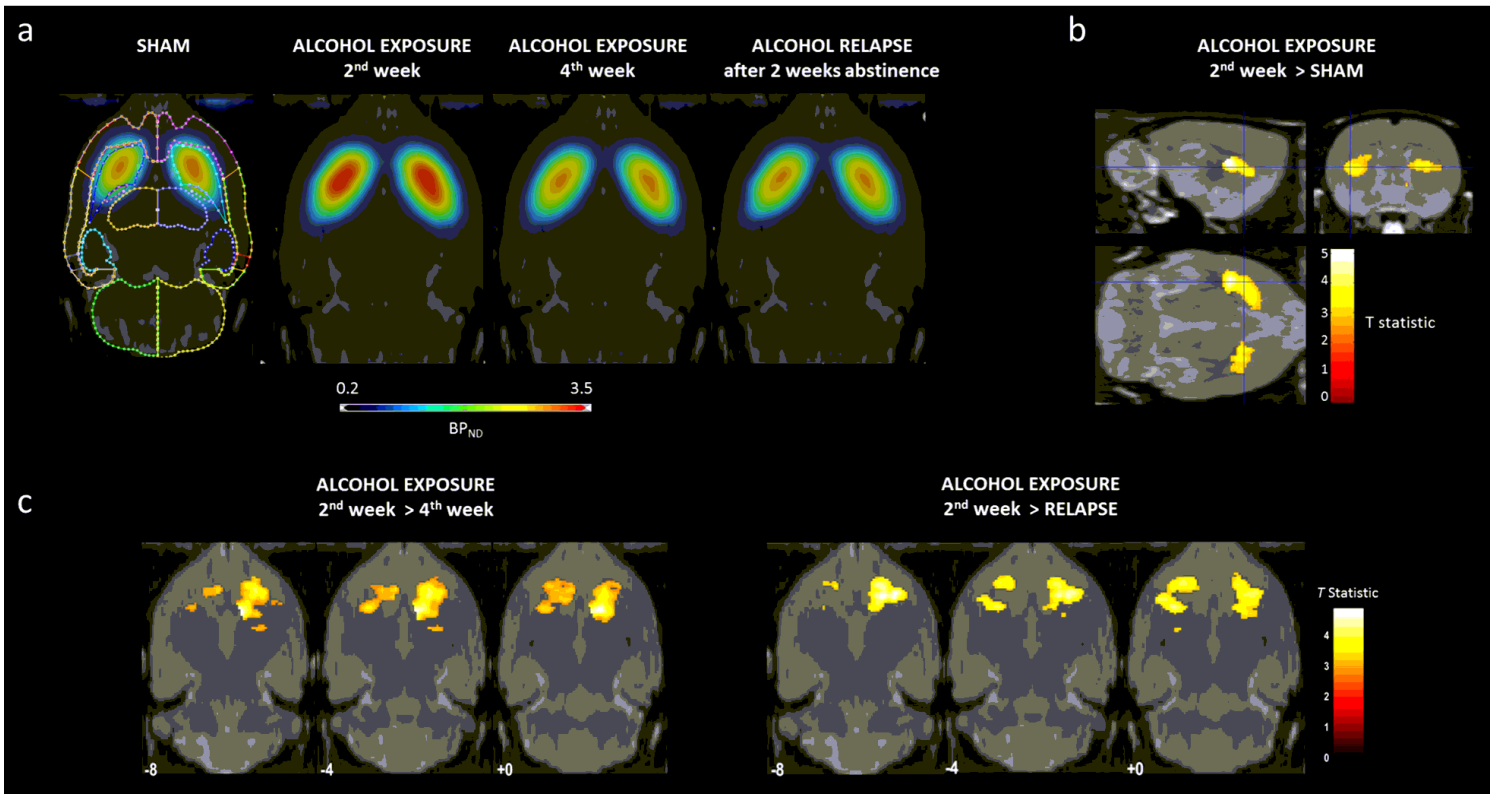

Figure 4

Phosphodiesterase 10a (PDE10A) availability changes at 2 and 4 weeks of alcohol exposure, and during the relapse phase. (a) Merged striatal PDE10A availability at the time points of control (sham), alcohol exposure week 2, alcohol week 4 and relapse, shows the initial increase of PDE10A availability in alcohol week 2 and its reversibility over alcohol week 4 and no increase at relapse conditions. Additionally, an illustrative example of the volumes-of-interest (VOI) map in Paxinos space is presented in Figure 4.a. (b) Brain sections show overlays of T-maps at the voxel level on the striatal regions with significantly increased PDE10A availability after 2 weeks of alcohol exposure, compared to sham. The intersection point is set to the Paxinos coordinate peak max (p = 2.5·10-4) located in the left caudate-putamen (x = -4.4 mm, y = 0.7 mm, z = 4.6 mm). (c) PDE10A decreased in a cluster located in the bilateral caudate-putamen and NuAc comparing 2 weeks and 4 weeks alcohol exposure as well as 2 weeks vs 2 weeks relapse alcohol exposure.

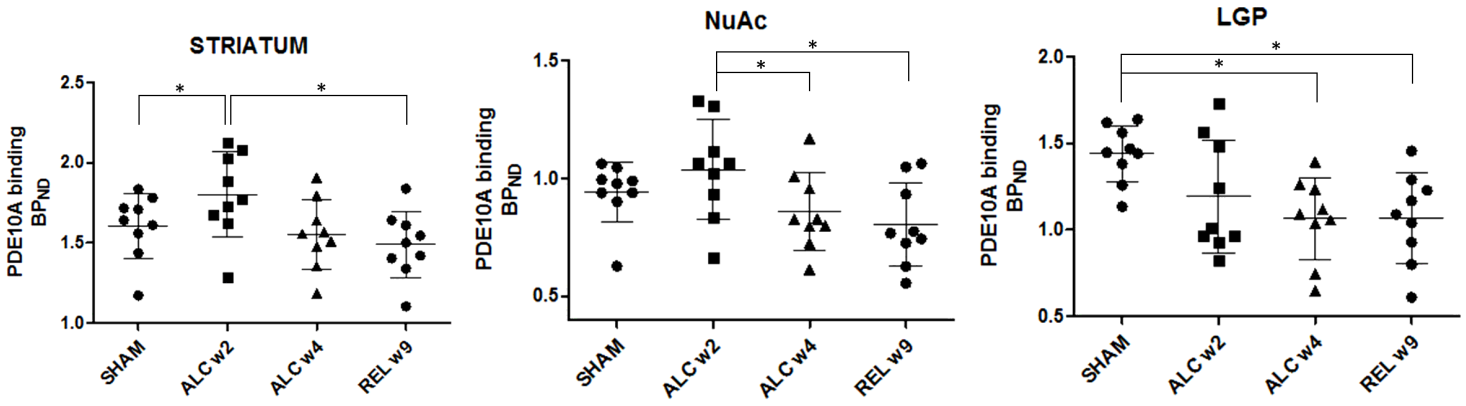

Figure 5

PDE10A binding in rats after 1 week of relapse compared to the sham control group. Brain sections show overlays of T-maps on the regions with significantly decreased PDE10A binding after one week of relapse, compared to the sham control group. The intersection point is set to the Paxinos coordinate located in the right globus pallidum (x = 3.0 mm, y = -0.9 mm, z = 5.8 mm, p = 0.001, T = 3.2). Significant clusters are indicated using a T-statistic color scale, which shows significance at the voxel level.

Supplementary Files

This is a list of supplementary files associated with this preprint. Click to download.

- PDE10AmicroPETinalcoholmodelSupplementaryInformation.docx